Entropy Fuzzy System Identification for the Dynamics of the Dragonfly-like Flapping Wing Aircraft

Fendy Santoso, Matthew A. Garratt, Sreenatha G. Anavatti, and Osama Hassanein

***Abstract*—In this work we present non-linear system identification for a class of the dragonfly-like flapping wing aircraft. We model the system in its vertical and all attitude loops (roll, pitch, and yaw) as well as its actuator dynamics. Based on a set of input-output data, obtained from first principle modelling; we perform the entropy fuzzy system identification to derive the open loop dynamics of the aircraft using the Mamdani Fuzzy inference method, which is more intuitive, despite being non-linear. This will make the proposed models well-suited to non-expert users (e.g. average drone operators). Our research indicates that the information entropy is very effective to maximize the system accuracy while avoiding overfitting problems. Through numerical simulation, we demonstrate the efficacy of the proposed fuzzy models as we can achieve reasonably good average modelling accuracy of around 90 % for all attitude loops.**

***Index Terms*—Non-linear System Identification, Entropy Fuzzy, Dragonfly-like Flapping Wing Aircraft.**

I. Introduction

The advent of intelligent robots has brought numerous advantages in modern societies to improve safety and productivity. For instance, robotic sensor networks can perform self-deployment to secure a protected region [1], [2], [3] while unmanned underwater vehicles (UUVs) are suitable for dangerous maritime and underwater explorations [4], [5]. Furthermore, the developments of unmanned aerial vehicles (UAVs), also colloquially known as drones, have numerous applications in both civilian and military domains (e.g. forest and wildlife monitoring [6], aircraft inspection [7], search and surveillance [8], law-enforcement [9], counter-drug operations [10], and smart cities [11], to name a few.)

Today, current research trends in aerial robotics have led to the developments of micro aerial vehicles (MAVs), which can be defined as a class of UAVs that have much smaller physical dimension ($<$15 cms) with a mass less than 90 grams [10]. Its light-weight design can substantially conserve in-flight power consumption leading to extended flight duration (longer endurance) and minimum downtime, lower noise, and also potential for low production costs [10], [12].

Mimicking avian aeromechanics, several researchers have developed flapping wing MAVs. For instance, a 60 mg insect scale MAV - with 3 cm wing span MAV in [13] as well as the 10 gram nano-hummingbird in [14] are some relevant examples of artificial birds. However, in this paper, we refer to the previous research conducted by Kok and Chahl in [15], where the authors developed a low cost simulation platform for a 40 gram flapping wing aircraft based on the concept of the quasi steady blade element model.

Inspired by four-wing insects, the flapping wing of our interest is known as the 'Dragonfly' MAV, which can offer numerous advantages compared to the conventional fixed or the rotary wing aircraft. The proposed system has a proficiency in three flight modes, namely, glide, hover, and agile maneuver, including (take-off, roll and yaw turns) [15], [16], [17]. Mimicking birds and insects, the system has the capability of pitching up at higher angles-of-attack and decelerating rapidly to approach the target [15]. Nonetheless, its small dimensions and low velocities may lead to aerodynamic challenges due to lower Reynolds number effects. However, this challenge can be overcome by flapping the wings to increase Reynolds number [10].

The system works based on the unsteady aerodynamics [10], achieved by creating upstroke and down-stroke movements of the wings. The size of the wing may be adjusted and rotated about the chord to achieve high degree of freedom. As the system flaps, the aircraft needs to make the correct angle-of-attack in order to be able to generate an optimum lift. Flapping wing aircraft offer diverse combinations of forces to support their motions. Although there are two basic ways of flying, such as flying with lift or with thrust; there are also some flying combinations using both lift and thrust.

Unlike fixed-wing aircraft that employ their wings to produce lift and engine to produce thrust; flapping wing aircraft can produce the combination of both forces simultaneously through complex relationships between the frequency, amplitude and phase relationships of the wing plunging and pitching motions. Interested readers may refer to [13], [14].

Owing to its unique airframe construction, flapping wing MAVs can also provide *natural camouflage* because of their resemblance to insects or birds. Thus, MAVs are very suitable for surveillance in military and law enforcement applications. Meanwhile, in agriculture, flapping wing MAVs have been developed to control the population of certain birds and to clear landfills and waste management sites of the unwanted birds. An example of this application is a remotely piloted robotic bird, known as 'rhobird,' an artificial prey bird, which is realistic enough to frighten the unwanted birds [18].

It is not currently possible to effectively control a flapping

Fendy Santoso, Matthew A. Garratt, and Sreenatha G. Anavatti are with the School of Engineering and Information Technology, The University of New South Wales, Canberra, ACT, 2612, Australia; Osama Hassanein is with the Abu Dhabi Polytechnic, Abu Dhabi, UAE. Corresponding author: Fendy Santoso, Email: F.Santoso@adfa.edu.au.

wing aircraft with manual human controls due to the high number of control variables and the required control bandwidth in addition to being heavily over-actuated. Thus, the system requires the availability of robust autopilot systems. While the performance of traditional control systems are still heavily reliant on the accuracy of the mathematical model, fuzzy systems allow simpler and more practical solutions for modelling and control of complex non-linear systems, in particular for the flapping wing aircraft of our interest. In addition, this paper also serves as an initial study towards the development of the *evolutionary* fuzzy controller for a flapping wing aircraft.

Known as the robust *universal* approximator [19], fuzzy systems allow complex systems to be approximated using a set of fuzzy 'If-Then' rules, allowing better robustness and flexibility, compared to the traditional model-based control systems, whose performance completely relies on the accuracy of the proposed mathematical model in the form of the transfer functions or the state space equations [20], [21]. It is clear that traditional mathematical models often fail to capture the entire behaviours of complex dynamical systems, such as those due to strong non-linearity and time-varying characteristics.

Meanwhile, there are other advantages of employing fuzzy systems for modelling and control of complex systems. Considering their *intuitive* nature [19], deeper insight into the behavior of the systems could be drawn, even from the perspective of the non-expert users (e.g. average drone operators). This way, non-specialist users could directly comprehend the characteristics of the proposed systems by examining their associated fuzzy rule-base, given they are sufficiently small and simple [19].

A. Related Work

Most current research in robotic aircraft still heavily focuses on fixed and rotary wing aircraft (e.g. quadcopter and helicopter [20], [22], [23]). Although some researchers have studied the mathematical models of the flapping wing aircraft [24], more studies are required to fully comprehend its dynamics, especially for the dragonfly model [15]. Many mathematical models seem to be very complicated and lack of practical consideration, such as those derived from first principle approaches [25], requiring complete knowledge of the forces applied in wings, body and tails, which may not be practical. Other non-linear approaches (e.g. Lagrangian [26]) employ complex non-linear differential equations, in which one needs to overly simplify several assumptions and constraints to be able to solve the equations.

To the best of our knowledge, none has employed the concept of the entropy *fuzzy* in robotic aircraft, despite their numerous potential benefits, such as the ability to prevent overfitting problems, while still maintaining reasonably high accuracy. Overfitting, such as being excessively complex relative to the characteristics of the data, which is a common problem in knowledge acquisition and data extraction [27], can lead to many disadvantages that may hinder the real-time applications of the control algorithms, especially for small UAVs (e.g. DI-MAVs). This will lead to poor predictive performance and computational expense.

Accordingly, the contribution of this paper, addressing current research gap, is to firstly develop accurate entropy fuzzy models, representing the non-linear dynamics of the DI-MAV along its four loops in addition to its actuator. We believe that our work can pave the way towards the development of fuzzy logic in modelling and control of flapping-wing aircraft (e.g. for its simplicity and computation, despite being non-linear) compared to other model based and non-linear system identification techniques. Using the well-known concept of the 'information entropy,' we can optimise the accuracy of the proposed fuzzy models while avoiding overfitting. We demonstrate the efficacy of our proposed fuzzy models in terms of its accuracy and simplicity.

The organisation of this paper is as follows. Section II depicts the physics, governing the dynamics of the DI-MAV while Section III describes the concept of the non-linear system identification, in particular the concept of the fuzzy entropy used in our system. Section IV highlights the efficacy of the proposed fuzzy model while Section V concludes this paper.

II. Dragonfly-Inspired Micro Aerial Vehicle (DI-MAV) Dynamics

This section discusses the physical laws, governing the dynamics of the flapping wing aircraft. We employ the quasi-steady state element as discussed in [15] to analyse the aerodynamic forces, which will later be combined with the environmental forces to determine the overall dynamics of the DI-MAV.

Firstly, the flapping angle ϕ of all four wings can be represented using the following equation:

$$\phi(t) = \phi_0 \cos(\pi f t), \tag{1}$$

where f indicates the flapping frequency, ϕ_0 denotes the flapping amplitude, and t indicates time. Moreover, the angle-of-attack α can be represented as follows:

$$\alpha = \alpha_m - \alpha_0 \sin(\omega t + \Delta\phi), \tag{2}$$

where $\omega = 2\pi f$ represents the angular flapping velocity, α_m indicates the mean angle-of-attack, α_0 denotes the amplitude of the pitching oscillation, and $\Delta\phi$ highlights the rotational phase. The schematic diagram, detailing the position of each actuator with respect to the rigid body is given in Fig. 1.

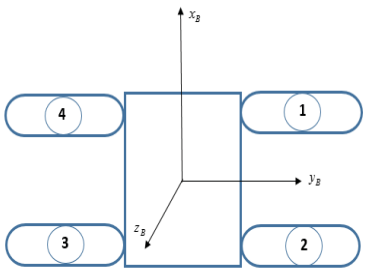

Fig. 1. An illustration of the flapping wing airframe in the body coordinate system. Numbered circles denote the position of the actuator controls.

According to Wang [28], [29], [30], the equations for the lift C_L, and the drag C_D coefficients as well as the rotational pressure C_r employed as the basis for calculating the flight dynamics can be presented as follows:

$$\begin{aligned} C_L &= 0.225 + 1.58\sin 2.13\alpha - 7.2 \\ C_D &= 1.92 - 1.55\cos 2.04\alpha - 9.82 \\ C_r &= \pi(0.75 - \hat{x}_0), \end{aligned} \tag{3}$$

where $\hat{x}_0$ is the rotational axis from the leading edge. Thus, the aerodynamics forces due to the translational and the rotational motions of the wings can be calculated as follows:

$$\begin{aligned} dL &= 0.5\rho V^2 C_L dS \\ dD &= 0.5\rho V^2 C_D dS \\ dF_{rot} &= C_r \rho c^2 U \dot{\alpha} dr, \end{aligned} \tag{4}$$

where L, D and S indicate lift, drag, and the surface area of the wing, respectively. Meanwhile, ρ indicates the density of the air, V and U represent the velocity due to wind speed and the translational velocity of the wing, and F_{rot} is the rotational force. Thus, the following vector summaries some important input variables or the flapping parameters of each wing: $u = [\beta\ f\ \phi_0\ \theta_m\ \theta_0\ \Delta\phi]^T$, where β indicates the stroke plane angle.

One important characteristics of the dragonfly flight is the phase relation between the fore-wings and the hind-wings, whose aerodynamic interactions may enhance the net vertical force, as opposed to the two independent wings [30]. Thus, the wings beat out of phase (counter-stroke) during steady hovering to slightly decrease the net vertical force, the force fluctuation, the body osculation as well as to minimise the aerodynamic power. Meanwhile, during take off the wings beat nearly in-phase.

While the amplitude and the frequency of the wing-beat plays an important role in creating the vertical take-off acceleration, the flapping amplitude and the stroke angle determine the roll and yaw rate, respectively. For instance, 10 % frequency increase will result in a $2g$ increase in vertical acceleration while an increase in the flapping amplitude of the left pair wing creates right roll of 1.76 rad/s within two beats. The decrease of the stroke plane angle of the left wing results in the averaged yaw rate of 2.54 rad/s within two wing beats [15].

Furthermore, the relation between environmental factors (e.g. the gravity and the wind) with respect to the body force vectors F can be defined as follows [31]:

$$\bar{F} = [F_x,\ F_y\ F_z] = m(a + \bar{\omega} \times \bar{V}_b), \tag{5}$$

where m represents the mass (kg), V_b indicates the velocity of the body frame (m/s), a denotes the acceleration (m/s^2). Likewise, the rotational dynamics of the rigid body frame with respect to the moments $[L\ M\ N]$ can be depicted as follows [31]:

$$\bar{M}_b = [L\ M\ N] = I\dot{\bar{\omega}} + \bar{\omega} \times I\bar{\omega}, \tag{6}$$

where I denotes the moment of inertia of the body.

III. Entropy Fuzzy System Identification

In this section, we will discuss the concept of the entropy fuzzy system identification, employed to model the dynamics of the DI-MAV.

A. Problem Statement

General problem statement of the non-linear system identification can be described using the following vector of measurements (7):

$$\hat{y}(k+1) = f\{u(k),...,u(k-m+1),y(k),y(k-1),...,y(k-n+1)\}, \tag{7}$$

where $\hat{y}(.)$ denotes the output of the identified model, $f\{.\}$ denotes the unknown function, m and n are the numbers of the past input u and output y data, respectively. We employ the concept of the black box modelling since the physical insight of the system is not understood *a-priori*, as apposed to the white box counterparts, where the dynamics of the system will be derived from first principle.

In terms of the system configuration, there are two major identification techniques, namely, the parallel and the series-parallel models. While the parallel model employs the output

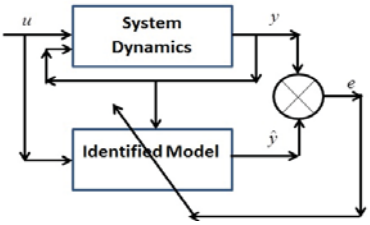

Fig. 2. Block diagram of the serial-parallel system identification. Prediction error e is defined as the difference between the output of the plant y and the output of the identified model $\hat{y}$, that is, $e = y - \hat{y}$ and is used to improve the accuracy of the model.

history from the identified model; series-parallel configuration, as in Fig. 2, employs true output of the plant directly as the input to the model. Thus, it is apparent that the series-parallel configuration can provide better robustness since the system does not propagate or accumulate the prediction error.

B. Entropy-Based Fuzzy System Identifier

In this section, we will discuss the concept of the entropy fuzzy, followed by the structure of the fuzzy network identifier. We also recall the concept of the back propagation of the error to fine-tune the parameters of the fuzzy membership functions.

1) The Concept of the Entropy Fuzzy: Entropy, in physics, generally refers to the degree of the *disorder* or uncertainty in closed dynamic systems. In the context of information theory, nonetheless, the concept of the Shannon's Entropy (named after Claude Shannon) indicates the expected value of the information contained in each message, which also indicates the limit of the best average length of the lossless encoding of an information source.

Intuitively, given the fuzzy set F defined on X with $F(x)$ and $G(X)$ represent the membership function and the overall fuzzy sets, defined on X; the entropy fuzzy of F, denoted

by $H(F)$ satisfies the following requirements [27]: (1) $H(F)$ will be minimum iff $\forall x \in X,\ F(x) = 0 \vee F(x) = 1$, (2) $H(F)$ will be maximum iff $\forall x \in X,\ F(x) = 0.5$. Maximum entropy implies more information will be received. Thus, it is desirable. Mathematically, Shannon's Entropy can be formulated as follows:

$$H(X) = -\sum_{i=1}^{n} P(x_i)\log_b\{P(x_i)\}, \tag{8}$$

where b is the base of logarithmic, normally $b = 2$. However, some commonly used values include $b = e$ and $b = 10$. The equation in (8) will be used as a threshold of decision, to determine whether it is necessary or not for the system to add a new rule. This way, one can make the most of the existing fuzzy rules and to avoid overfitting issues.

Within our research group, the authors in [32] implemented the concept of the entropy-based fuzzy modelling and control techniques for an underwater vehicle. The process consists of two major steps. While the off-line step employs the concept of entropy to avoid over fitting while still maintaining reasonably good accuracy, the back propagation of the error is employed to fine tune the parameters of the fuzzy systems.

More specifically, the entropy will be determined based on the *firing* strength of each rule, indicating the association of the incoming pair to a certain cluster. Accordingly, the maximum entropy can be calculated as follows:

$$H_{L_{max}} = \max_{1\le X\le R(t)} H_L, \tag{9}$$

where $R(t)$ indicates the number of the existing rules at time kT.

The error between the data employed in the structure generating phase and the output of generated model will be calculated. Should the design objectives are met, the generated model will enter the next phase, otherwise, H_L as in (9) will be adjusted. A new rule will be generated if $H_{L_{max}} \le \bar{H}_L$, where $\bar{H}_L$ denotes a predefined threshold. Thus, lower $\bar{H}_L$ indicates fewer rules, while higher $\bar{H}_L$ denotes the requirement of having more rules. The selection of the threshold of the entropy will accordingly affect the accuracy of the modelling.

After the generation of new rules, the next step is to define the initial mean and variance for that membership functions and the consequent part, namely, c_{ji}, σ_{ji}, b_{ji} and σ_i where c_{ji} and σ_{ji} denote the centre and the width of the Gaussian membership functions of x_i while b_{ji} and σ_i denote the parameters of the consequent layer. The process will be repeated until all the input-output data has been fully examined. The system employs the supervised learning technique by means of the back-propagation technique.

2) Fuzzy Network Identifier: Unlike conventional mathematical modelling techniques, fuzzy systems can be regarded as a method of describing the dynamics of complex systems by means of the linguistic 'If-Then' rules:

$$R^{(1)}: \textbf{IF}(x_1 \textit{ is } F_1^1, \textit{ and ... and } x_n \textit{ is } F_n^1) \textbf{ Then } y_1 \textit{ is } G^1, \tag{10}$$

where $x \in U^n$ and $y \in R^m$ indicate the input and output variables of the fuzzy system, respectively, while A and B are the labels of the fuzzy sets in U and R domains, respectively.

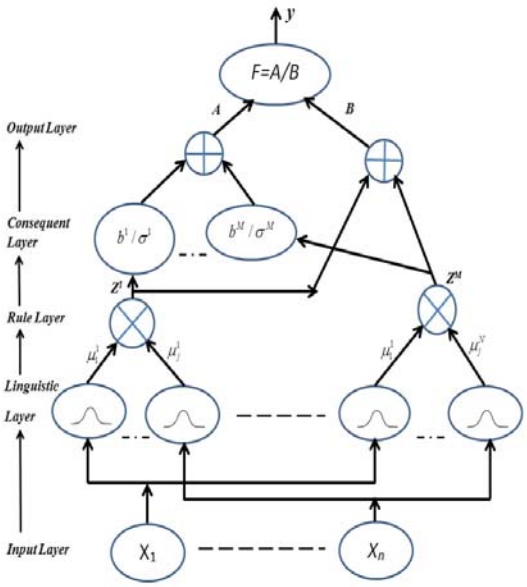

Fig. 3. The structure of the five layers of the Mamdani fuzzy network identifier, employed to model the dynamics of the flapping wing aircraft.

As discussed in [33], fuzzy systems can be represented in the form of five layers of feed-forward network, as seen in Fig. 3. While the first layer, as in (10), passes the crisp input to the subsequent layer, the calculated membership in layer two can be presented as follows:

$$L_{ji}^{(2)} = \exp\Big(-0.5\frac{(x_i - c_{ji})^2}{\sigma_{ji}^2 + \varepsilon}\Big), \tag{11}$$

where $\varepsilon > 0$ indicates a small constant, so that given $\sigma_{ij} = 0$, the function is still well-defined. Given (11), the output function of the third layer can be described as follows:

$$L_j^{(3)} = \prod_{i=1}^{N} L_{ji}^{(2)}, \tag{12}$$

where $L_j^{(3)}$ indicates the firing strength of the corresponding rule. Considering (12), the output of layer 4, known as the *consequent* layer can be computed as follows:

$$L_j^{(4)} = b_i \frac{L_j^{(3)}}{\sigma_i^2 + \varepsilon}. \tag{13}$$

Finally, the outcome of layer 5 can be described as follows:

$$\hat{y}(x) = \frac{\sum_{j=1}^{M} b_j \Big[\prod_{i=1}^{N} \frac{\exp\Big(-0.5\frac{(x_i - c_{ji})^2}{\sigma_{ji}^2+\varepsilon}\Big)}{\sigma_i^2+\varepsilon}\Big]}{\sum_{j=1}^{M} \Big[\prod_{i=1}^{N} \frac{\exp\Big(-0.5\frac{(x_i - c_{ji})^2}{\sigma_{ji}^2+\varepsilon}\Big)}{\sigma_i^2+\varepsilon}\Big]}, \tag{14}$$

where N denotes the number of fuzzy rules. The free parameters of the fuzzy model in (14), updated in the adaptation process, are c_{ji}, σ_{ji}, b_j, and σ_i.

3) The Back Propagation of Error: We employ the gradient-based learning method, known as the back propaga-

tion of the error, adjusting the parameters of the system based on the negative gradient of a certain cost function (15).

$$J = \frac{1}{2}\sum_{i=1}^{q}(\hat{y}(k+1) - y(k+1))^2, \tag{15}$$

where $\hat{y}(k)$ denotes the predicted output and $y(k)$ highlights the actual output of the system. Meanwhile, fuzzy parameters $z(k)$ can be optimised using the following rules:

$$z(k+1) = z(k) - \alpha\frac{\partial e}{\partial z}, \tag{16}$$

where α indicates the rate of the learning, determining the stability and the convergence of the system.

Considering (16), we train the fuzzy systems and update b_i as follows:

$$b(k+1) = b(k) - \alpha\frac{L_j^{(3)}}{B_i\sigma_{ij}^2 + \varepsilon}, \tag{17}$$

while σ_i is optimised as follows:

$$\sigma_i(k+1) = \sigma_i(k) - \left\{\alpha\frac{b_i - y}{B_i}\right\}\left\{\frac{L_j^{(3)}}{(\sigma_{ji}^2+\varepsilon)^2}\right\}(-2\sigma_{ji}). \tag{18}$$

Moreover, c_{ji} is defined as follows:

$$c_{ji}(k+1) = c_{ji}(k) - \alpha\left\{\frac{b_i - y}{B_i}\right\}\left\{\frac{L_j^{(3)}}{\sigma_{ji}^2+\varepsilon}\right\}\left\{\frac{x_j - c_{ji}}{\sigma_{ji}^2+\varepsilon}\right\}, \tag{19}$$

while σ_{ji} is trained as follows:

$$\sigma_{ji}(k+1) = \sigma_{ji}(k) - \alpha\left\{\frac{b_i - y}{B_i}\right\}\left\{\frac{L_j^{(3)}}{\sigma_{ji}^2+\varepsilon}\right\}\left\{\frac{2(x_i - c_{ji})^2}{(\sigma_{ji}^2+\varepsilon)^2}\right\}\sigma_i, \tag{20}$$

where $B_i = \sum_{i=1}^{N}\frac{L_j^{(3)}}{\sigma_i^2+\varepsilon}$. In what follows, we will study the performance of the entropy fuzzy system identification to model the dynamics of the DI-MAV.

IV. System Performance

In this section, we study the effectiveness of the proposed entropy fuzzy models. We first study the dynamics of the actuators before moving into the open loop dynamics of the rigid body of the flapping wing aircraft in its vertical and all attitude loops. For the purpose of data collection, we employ a sampling rate of 100 Hz.

A. The Aerodynamic Force of the Actuator

The actuator of the DI-MAV aircraft can be regarded as a multi-input, multi-output system since it has 6 major inputs: $u = [\beta\ f\ \phi\ \theta_m\ \theta_0\ \Delta\phi]^T$ (see Section II) and 2 major outputs in terms of the actuator forces F_a, namely, $F_a = [F_{a_x}\ F_{a_z}]^T$, since $F_{a_y} \approx 0$. However, for each actuator, F_{a_z} is the most dominant component compared to F_{a_x}. Also, it should be pointed out that flapping amplitude and frequency are the two most dominant inputs, compared to the rest, namely, angle of attack and stroke plane whose effects are negligible.

1) The Dynamics of the Vertical Force F_{a_z}: To perform the fuzzy system identification of the F_{a_z}, we first set the target entropy to 0.178 and vary both f and ϕ_0 while other variables are set to be constant. We record the average value of the vertical output forces F_{a_z}. The identification outcome for the mean of the F_{a_z} is given by Fig. 4 while the entropy fuzzy model (system parameters) for the mean of the vertical force F_{a_z} are given by Fig. 5. As indicated, the prediction of our fuzzy model is highly accurate as it can closely mimic the actual force output of the actuator. For the target entropy

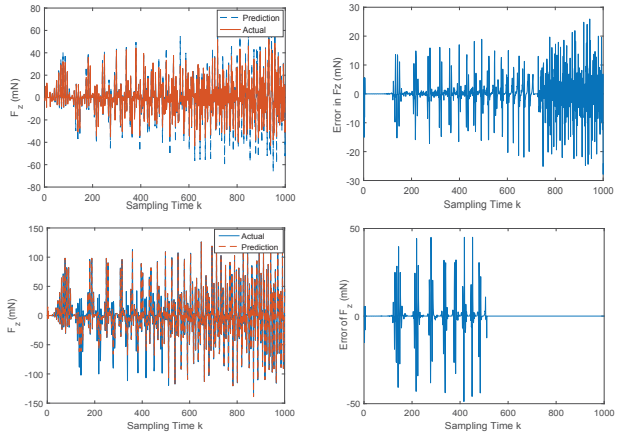

Fig. 4. (a) Top left: Modelling of the vertical force of an actuator along z-axis under varying frequency between 5.5-6.5 Hz and varying ϕ_0 as given by a chirp signal with an amplitude of $\pm$ 30 and a sweeping frequency up to 5 Hz, (b) Top right: modelling error of F_z, (c) Bottom Left: The validation of F_z where we feed the system with a set of different signal up to 7 Hz and varies its amplitude as given by the chirp signal with a sweeping frequency up to 8 Hz, (d) Bottom right: the validation error of F_z.

$\overline{H}_L$ of 0.007, we can achieve a fuzzy system containing 18 membership functions as indicated in Fig. 5. The proposed

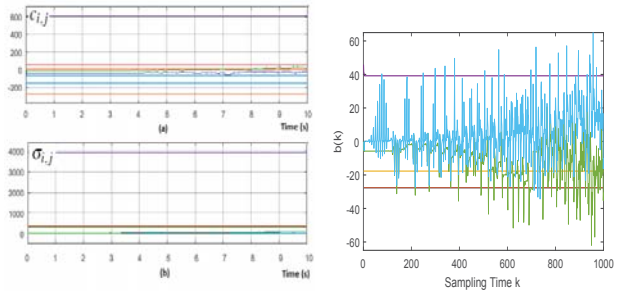

Fig. 5. The evolutionary process of our fuzzy parameters: (a,b) Left: $\sigma_{i,j}$ and $c_{i,j}$ as a function of k, (c) Right: b_j as a function of time in seconds.

model performs well as indicated by its accuracy.

2) The Dynamics of the Horizontal Force F_{a_x}: In this section, we will model the mean of the horizontal force F_{a_x} as a function of the similar actuator inputs. We decrease the target entropy $\overline{H}_L$ into 0.002 to achieve fewer membership functions. The proposed fuzzy model now only contains 8 membership functions as indicated in Fig. 7. Accordingly, we can achieve simpler fuzzy model to reduce the computational burden of the system.

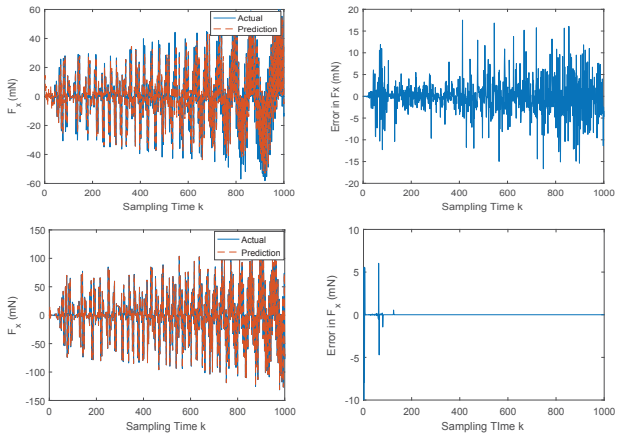

Fig. 6. (a) Top left: modelling of the horizontal force of an actuator along x-axis under the frequency between 5.5-6.5 Hz and varying ϕ_0 as given by the chirp signal with an amplitude of $\pm$ 30 deg and with a sweeping frequency up to 5 Hz, (b) Top right: the modelling error of F_x, (c) Bottom left: validation signal of the F_x, where we feed the system with a set of different chirp signal up to 7 Hz and varying amplitude as given by the chirp signal with a sweeping frequency up to 8 Hz, (d) Bottom right: the validation of the error of F_x.

The resulting fuzzy parameters for the input membership function $c_{i,j}$, $\sigma_{i,j}$, and the output membership function b_j are given in Fig. 7. This way, one can also claim that the algorithm

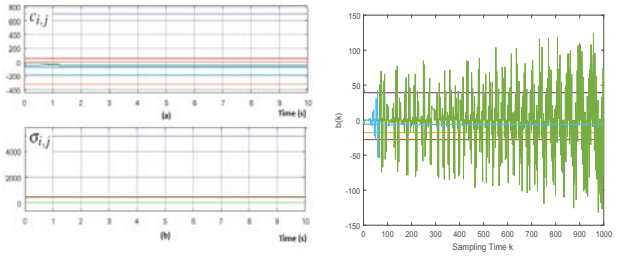

Fig. 7. (a, b) left: $\sigma_{i,j}$ and $c_{i,j}$ as a function of k given $T_s = 0.01s$, and (c) Right: b_j as a function of time in seconds.

is sufficiently robust in the face of the frequency variation. The performance of the entropy fuzzy system identification is fairly stable in the higher frequency regions as in the lower frequency counterparts. This will bring more confidence about the feasibility of the identification algorithm to be employed in the real-time control systems. In this scenario, the accuracy of the proposed model is greater than 80 %.

B. Rigid Body Dynamics

The DI-MAV of our interest has four actuators and each actuator, as earlier discussed, can be regarded as a 6 input system. Thus, the overall rigid body dynamics of our DI-MAV has 24 inputs with 6 degree of freedom as the output, namely, $y = [V_{b_x}\ V_{b_y}\ V_{b_z}\ \omega_{b_x}\ \omega_{b_y}\ \omega_{b_z}]^T$. However, to simplify the analysis we will consider the frequency, amplitude, and phase as the most dominant input. The output of interest is given by the vertical velocity V_{b_z}, and the attitude of the aircraft $[\phi\ \theta\ \psi]^T$, representing the roll, pitch, and yaw, respectively.

1) Vertical Velocity Dynamics: To model the v_{b_z}, we apply the same ϕ_0 for each actuator, which is fed by the same chirp signal. We set the target entropy $\overline{H}_L = 0.05$. We also consider the worst-case scenario, where the input signals for modelling is made different from the input signal we employ for validation. For each actuator, the frequency of the chirp signal is set around 5 Hz for modelling and around 6 Hz for validation. Likewise, we set a chirp signal with an amplitude of $\pm$70 deg, while for validation we adjust it to become $\pm$60 deg. To make it more realistic we introduce Gaussian noise of 0.01 Watt in both chirp signals.

While the quality of the prediction and the validation performance of the V_{b_z} can be found in Fig. 8, the adaptation process of all fuzzy parameters in all membership functions can be obtained in Fig. 9. In what follows, we will model

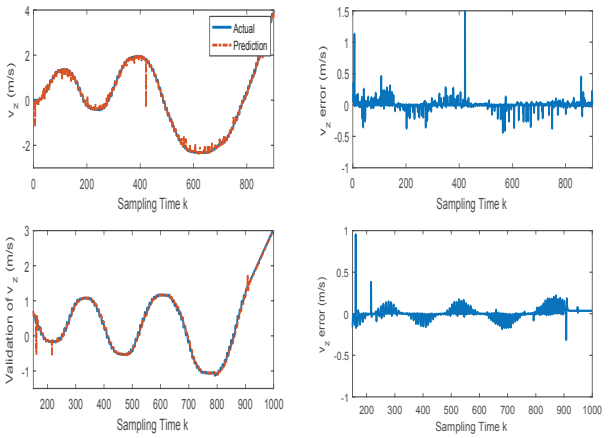

Fig. 8. (a) Top: modelling of the vertical velocity v_z of the rigid body of the aircraft under varying f and ϕ_0 (b) Bottom: the validation outcome of the proposed fuzzy model.

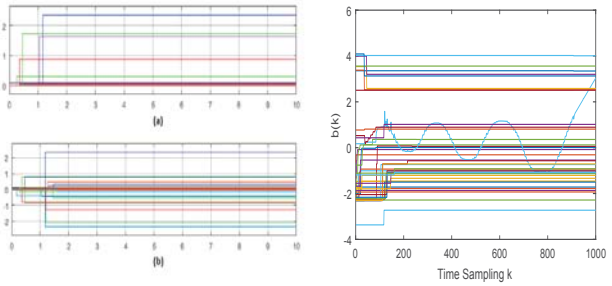

Fig. 9. The optimisation process of the fuzzy parameters of the v_{b_z} with 41 membership functions.

the dynamics of the attitude loops, namely, the roll, pitch, and yaw.

2) Roll Dynamics: For the purpose of data collection, we need to generate an oscillating roll to comprehensively capture the dynamics of the system. We will apply a couple of the inverse chirp signals with a magnitude of 15 deg. Thus, the input of the right actuators (no. 3 and 4) is in the opposite sign of the input of the left actuators (no. 1 and 2). Furthermore, we set the input flapping frequency $f = 5-6\ Hz$. Likewise, for validation, we do a similar thing, except we

change the magnitude of the amplitude to become 25 deg and with the sweeping rate of the chirp signal around 6-7 Hz. With $\overline{H}_L$=0.01, we can achieve as few as 6 membership

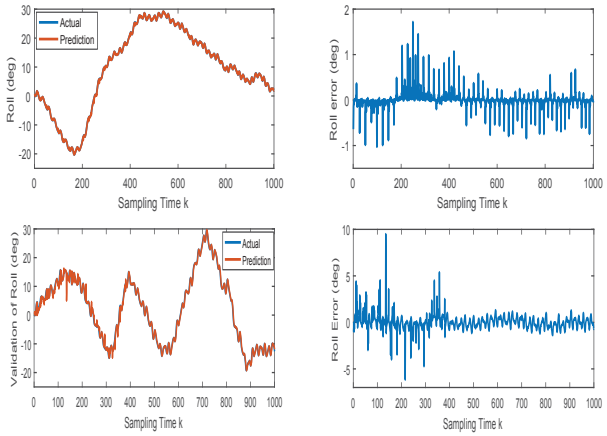

Fig. 10. Modelling the dynamics of the roll loop ϕ of the rigid body under varying f and ϕ_0.

functions only, whose parameters in time are given in Fig. 11. Overall, we can achieve a very good model whose accuracy is highlighted in Fig. 10 with a validation accuracy of 92.5 %.

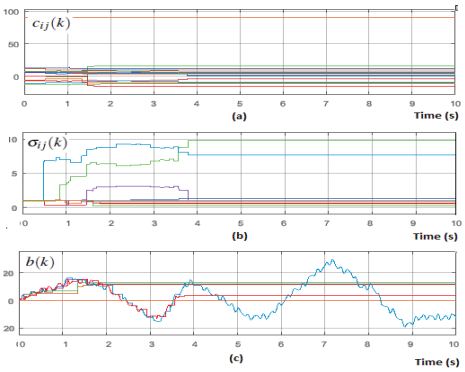

Fig. 11. Fuzzy parameters of the roll loop as represented by (a) $\sigma_{i,j}$, (b) $c_{i,j}$ as a function of k, and (c) b as a function of sampling time k.

3) Pitch Dynamics: As with the roll dynamics, we create an oscillating pitch by applying different inputs e.g. front actuator (no. 1 and 4) with respect to the back actuator (no. 2 and 3), see Fig. 1. This can be achieved by setting a different amplitude and frequency in the inverse pair, similar to the case of the roll loop. To obtain the fuzzy model with fewer membership functions, we set $\overline{H}_L$=0.001. This way, we end up having a fuzzy model, comprising of three fuzzy membership functions as given in Fig. 13. We should point out that the accuracy of both modelling and validation, as given by Fig. 12, is reasonably good. This indicates the effectiveness of the proposed model, despite the system only employs 3 membership functions.

4) Yaw Dynamics: In this section, we will discuss the dynamics of the yaw loop. To control yaw, we can use either: phase, amplitude, frequency or any combination of them. Unlike the roll and pitch, we choose a pair of actuator in

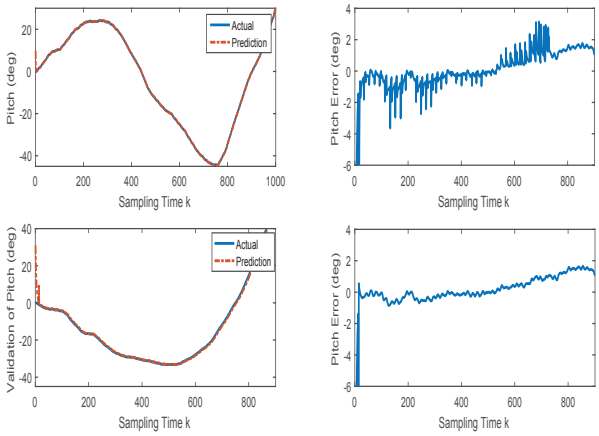

Fig. 12. Modelling of the pitch θ of the rigid body under varying f and ϕ_0.

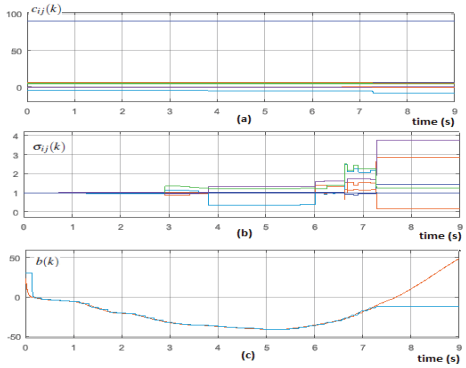

Fig. 13. Fuzzy parameters of the pitch loop as represented by (a) $\sigma_{i,j}$, (b) $c_{i,j}$, and (c) b as a function of k.

the diagonal position, namely, the actuators (1,3) to interact with the force produced by another pair of actuators (2,4) to create a sufficient yaw moment. The performance of the proposed fuzzy model is given in Fig. 14. With $\overline{H}_L = 0.25$,

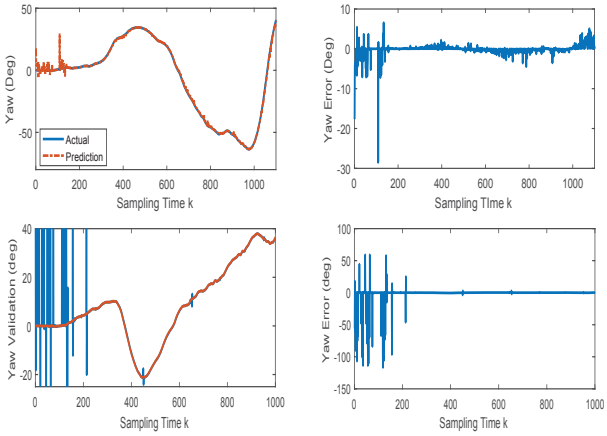

Fig. 14. Modelling of the yaw ψ of the rigid body under varying ϕ_0 and θ.

we acquire a fuzzy model with 34 membership functions, achieving modelling accuracy of around 98 %.

As can be seen, the system can achieve reasonably good

accuracy as it can adapt to the totally new input signal during the validation process.

V. Conclusion

We have performed non-linear system identification for a class of the dragon-fly inspired micro aerial vehicles. Leveraging on the benefits of the information entropy, we come up with highly accurate fuzzy models with accuracy $\geq 90\%$ for all attitude loops.

The proposed fuzzy models are also very computationally efficient since they can accurately represent the non-linear dynamics of the flapping wing aircraft with only as few as three membership functions only given the complex nature of the dragonfly-like flapping wing aircraft, which can be regarded as a 12 input rigid body system. The ability to avoid overfitting is another advantage of the entropy fuzzy system. This feature is critical for real time applications, especially for small aircraft, where we are often faced by the limitation of the on-board computer.

Owing to the nature of the Mamdani fuzzy system which is knowledge-based, the proposed model is also known for its transparency, despite being non-linear; making it easier for the average drone operators to get the message. Our research also indicates the robustness of the proposed model in the face of parameter changes and frequency variations, an important feature for robust control systems.

Acknowledgment

This research was supported by the Defence Science and Technology Organisation (DSTO), Australia.

References

[1] F. Santoso. A new framework for rapid wireless tracking verifications based on optimized trajectories in received signal strength measurements. *IEEE Trans on Systems, Man and Cybernetics: Systems*, 45(11):1424–1436, November 2015.

[2] F. Santoso. Range-only distributed navigation protocol for uniform coverage in wireless sensor networks. *IET Wireless Sensor Systems*, 5(1):20–30, February 2015.

[3] F. Santoso. A decentralised self-dispatch algorithm for square-grid blanket coverage intrusion detection systems in wireless sensor networks. In *Vehicular Technology Conference (VTC Fall)*, 2011.

[4] G. Ferri, A. Munafo, and K. D. LePage. An autonomous underwater vehicle data-driven control strategy for target tracking. *IEEE Journal of Oceanic Engineering*, pages 1–21, January 2018.

[5] M. M. Maia, D. A. Mercado, and F. J. Diez. Design and implementation of multirotor aerial-underwater vehicles with experimental results. In *IEEE/RSJ International Conference on Intelligent Robots and Systems (IROS)*, pages 961–966, Vancouver, BC, 2017.

[6] J. Paneque-Glvez, M. K. McCall, B. M. Napoletano, S. A. Wich, and L. P. Koh. Small drones for community-based forest monitoring: An assessment of their feasibility and potential in tropical areas. *Forests*, 5(6):1481–1507, 2014.

[7] F. Santoso, M. A. Garratt, M. R. Pickering, and M. Asikuzzaman. 3D-mapping for visualisation of rigid structures: A review and comparative study. *IEEE Sensors Journal*, 16(6):1484–1507, March 2016.

[8] D. Kingston, S. Rasmussen, and L. Humphrey. Automated UAV tasks for search and surveillance. In *EEE Conference on Control Applications (CCA)*, pages 1–8, Buenos Aires, 2016. 2016.

[9] M. Hlas and J. Straub. Autonomous navigation and control of unmanned aerial systems in the national airspace. In *IEEE Aerospace Conference*, pages 1–7, 2016.

[10] T. J. Mueller and J.D.De Laurier. *Fixed and Flapping Wing Aerodynamics for Micro Aer Vehicle Applications*, volume 195, chapter An overview of Micro Air Vehicle Aerodynamics, pages 1–12. AIAA, Reston, VA, 2001.

[11] A. Giyenko and Y. I. Cho. Intelligent UAV in smart cities using iot. In *16th International Conference on Control, Automation and Systems (ICCAS)*, pages 207–210, 2016.

[12] F. Santoso, M. A. Garratt, and S. G. Anavatti. Visual inertial navigation systems for aerial robotics: Sensor fusion and technology. *IEEE Transactions on Automation Science and Engineering*, 14(1):260–275, January 2017.

[13] R. J. Wood. Design, fabrication, and analysis of a 3DOF, 3cm flapping-wing MAV. In *IROS IEEE/RSJ International Conference on Intelligent Robots and Systems*, pages 1576–1581, 29 October - 2 November 2007.

[14] M. Keennon, K. Klingebiel, H. Won, and A. Andriukov. Development of the nano hummingbird: A tailless flapping wing micro air vehicle. In *50th AIAA Aerospace Sciences Meeting including the New Horizons Forum and Aerospace Exposition*, Nashville, Tennessee., 2012.

[15] J. M Kok and J. S. Chahl. A low cost simulation platform for flapping wing MAVs. In *Proc of SPIE: Bioinspiration, Biomimetics, and Bioreplication*, volume 9429, 2015.

[16] J. Chahl, G. Dorrington, S. Premachandran, and A. Mizutani. The dragonfly flight envelope and its application to micro UAV research and development. In *8th IFAC Symposium on Intelligent Autonomous Vehicles*, volume 46, page 231234. IFAC, June 2013.

[17] A. Mizutani, J. S. Chahl, and M. V. Srinivasan. Insect behaviour: Motion camouflage in dragonflies. *Nature*, 423(6940):604–604, June 2003.

[18] W. Straatman. Developing an autopilot for the peregrine falcon robird. Technical Report 021RAM2014, University of Twente, Netherland, October 2014.

[19] Q. Zhang and M. Mahfouf. Fuzzy modelling using a new compact fuzzy system: A special application to the prediction of the mechanical properties of alloy steels. In *Proceedings of the IEEE International Conference on Fuzzy Systems*, pages 1041–1048, Taipei, 2011. IEEE.

[20] M. Liu, G. Egan, and F. Santoso. Modeling, autopilot design, and field tuning of a UAV with minimum control surfaces. *IEEE Trans on Control Systems Technology*, 23(6):2353–2360, November 2015.

[21] F. Santoso, M. Liu, and G. Egan. H_2 and H_∞ robust autopilot synthesis for longitudinal flight of a special unmanned aerial vehicle: a comparative study. *IET Control Theory Appl.*, 2(7):583–594, 2008.

[22] F. Santoso, M. Garratt, and S. Anavatti. Fuzzy logic-based self-tuning autopilots for trajectory tracking of a low cost quadcopter. In *International Conference on Advanced Mechatronics, Intelligent Manufacture, and Industrial Automation*, 2015.

[23] F. Santoso, M. Garratt, and S. G. Anavatti. Adaptive neuro-fuzzy inference system identification for the dynamics of the AR.drone quadcopter. In *Proceedings of the Fourth International Conference on Sustainable Energy Engineering and Applications*. IEEE, October 2016.

[24] R. Y. Krashanitsa, D. Silin, S. V. Shkarayev, and G. Abate. Flight dynamics of a flapping-wing air vehicle. *International Journal of Micro Air Vehicles*, 1(1):35, 49 2009.

[25] B. P. Malladi, R. Y. Krashanitsa, D. Silin, and S. V. Shkarayev. Dynamic model and system identification procedure for autonomous ornithopter. In *3rd US-European Competition and Workshop on Micro Air Vehicle Systems (MAV07) and European Micro Air Vehicle*, France, September 2007.

[26] W. Buler, L. Loroch, K. Sibilski, and A. Zyluk. Modeling and simulation of the nonlinear dynamic behaviour of a flapping wwing micro-aerial-vehicle. In *42nd AIAA Aerospace Sciences Meeting and Exhibit*, pages 1–9, Nevada, January 2004. AIAA.

[27] X-Z Wang and C.-R. Dong. Improving generalization of fuzzy IF-THEN rules by maximizing fuzzy entropy. *IEEE Transactions on Fuzzy Systems*, 17(3):556–567, June 2009.

[28] Z. J. Wang. The role of drag in insect hovering. *Journal of Experimental Biology*, 207(23):4147–4155, August 2004.

[29] Z. J. Wang. Dissecting insect flight. *Annual Review of Fluid Mechanics*, 37:183–210, 2005.

[30] Z. J. Wang and D. Russell. Effect of forewing and hindwing interactions on aerodynamic forces and power in hovering dragonfly flight. *Physical Review L*, 99(14):148101, October 2007.

[31] J. R. Raol and J. SIngh. *Flight mechanics modelling and analysis*. CRC Press, 2008.

[32] O. Hassanein, S. G. Anavatti, and T Ray. *On-Line Adaptive Fuzzy Modeling and Control for Autonomous Underwater Vehicle*, volume 480, chapter Recent Advances in Robotics and Automation, pages 57–70. Springer, May 2013.

[33] L.-X. Wang. *Adaptive Fuzzy Systems And Control Design And Stability Analysis*. Englewood Cliffs, 1994.